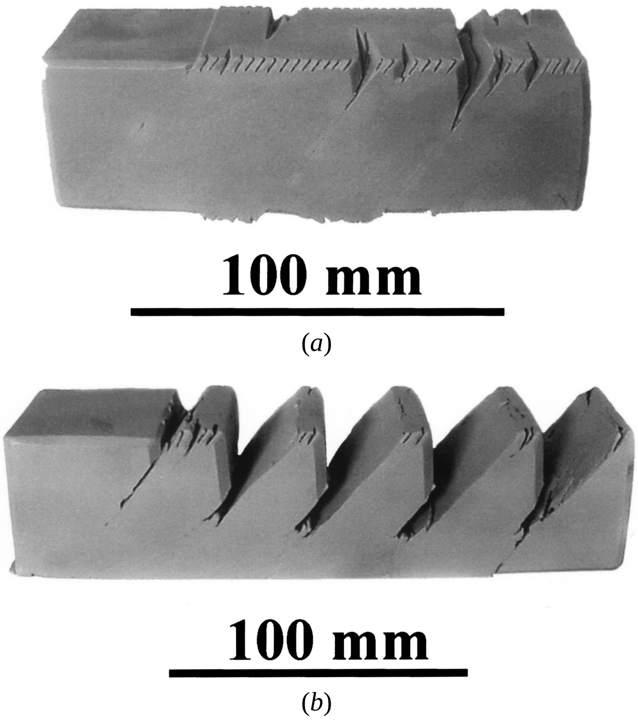

Fig. 2—Macrographs of aluminum alloy 2024-T851 samples after room-temperature ECAE at a ram speed of (*a*) 0.25 mm/s or (*b*) 25.4 mm/s.

at two different ram speeds are shown in Figure 2. At the lower ram speed (0.25 mm/s), corresponding to a strain rate of approximately 0.01 s^{-1}, cracking was noted to a depth of approximately 2.5 mm from the top surface. From the analysis in Reference 6, the tensile damage imposed during a single ECAE pass of a perfectly plastic material through a 90 deg die varies from approximately 0.25 at the top surface to zero at a depth equal to one-fifth of the cross section. Thus, the observed depth of cracking does correlate approximately to that at which the tensile damage factor drops below the critical value of $\sim$0.10 determined from the tension tests.

The ECAE sample deformed at the higher ram speed of 25.4 mm/s (corresponding to an average strain rate of 1 s^{-1}), shown in Figure 2(b), revealed evidence of both gross fracture and shear failure. The fracture was evidenced by wide gaps between "sawteeth" that separated workpiece segments. It may be concluded that the high value of the flow localization parameter at this strain rate (Table I) led to the formation of shear bands during ECAE and that cracking due to tensile damage at the top sample layers propagated along the shear bands.

The results of this investigation verify that two distinct types of failure may occur during ECAE. The specific type depends on two material properties—the alpha parameter in shear, γ'/m, and the critical tensile damage factor from the Cockcroft-and-Latham criterion. Depending on the specific values of these properties, fracture, shear localization, or a combination of the two may occur.

This work was conducted as part of the in-house research activities of the Metals Processing Group of the Air Force Research Laboratory's Materials and Manufacturing Directorate. The support and encouragement of the laboratory management and the Air Force Office of Scientific Research (Dr. C.S. Hartley, program manager) are gratefully acknowledged. Three of the authors (PNF, JB, and TB) were supported under the auspices of Air Force Contract No. F33615-96-C-5251.

REFERENCES

1. V.M. Segal, V.I. Reznikov, A.E. Drobyshevskiy, and V.I. Kopylov: *Russ. Metall.*, 1981, vol. 1, pp. 99-105.
2. V.M. Segal: *Proc. 5th Int. Aluminum Technology Seminar*, Aluminum Association, Washington, DC, 1992, vol. 2, pp. 403-08.
3. R.Z. Valiev, R.K. Islamgaliev, and I.V. Alexandrov: *Progr. Mater. Sci.*, 2000, vol. 45, pp. 103-89.
4. D.P. DeLo and S.L. Semiatin: *Metall. Mater. Trans A*, 1999, vol. 30A, pp. 1391-1402.
5. S.L. Semiatin, V.M. Segal, R.L. Goetz, R.E. Goforth, and T. Hartwig: *Scripta Metall. Mater.*, 1995, vol. 33, pp. 535-40.
6. S.L. Semiatin, D.P. DeLo, and E.B. Shell: *Acta Mater.*, 2000, vol. 48, pp. 1841-51.
7. R.L. Goetz and S.L. Semiatin: Air Force Research Laboratory, Materials and Manufacturing Directorate, Wright-Patterson Air Force Base, OH, unpublished research, 1994.
8. S.L. Semiatin and J.J. Jonas: *Formability and Workability of Metals*, ASM, Materials Park, OH, 1984.
9. M.G. Cockcroft and D.J. Latham: *J. Inst. Met.*, 1968, vol. 96, pp. 33-39.

Effect of Texture Changes on Flow Softening during Hot Working of Ti-6Al-4V

S.L. SEMIATIN and T.R. BIELER

The modeling of deformation processes requires accurate descriptions of plastic flow (constitutive) behavior and microstructure evolution. Constitutive equations are typically one of two types. For the first, or engineering, approach a phenomenological relation between stress, strain, strain rate, and temperature is derived from simple workability tests. These relations work well when applied within the range of measurements, but are usually incapable of describing flow response during changes in strain path or temperature, for example. It is only with the second form of constitutive relation, based on internal-state or microstructural variables, that such effects can be taken into account. Although often more complex, the physically more realistic, state-variable descriptions of flow provide important insight into the close coupling of microstructure/texture evolution and constitutive behavior. Thus, extensive work has been conducted to develop such descriptions for common engineering alloys such as those based on aluminum or iron.[1,2]

S.L. SEMIATIN, Senior Scientist, Materials Processing/Processing Science, is with Air Force Research Laboratory, Materials and Manufacturing Directorate, AFRL/MLLM, Wright-Patterson Air Force Base, OH 45433-7817. T.R. BIELER, Associate Professor, is with the Department of Materials Science and Mechanics, Michigan State University, East Lansing, MI 48824-1226.
Manuscript submitted August 16, 2000.

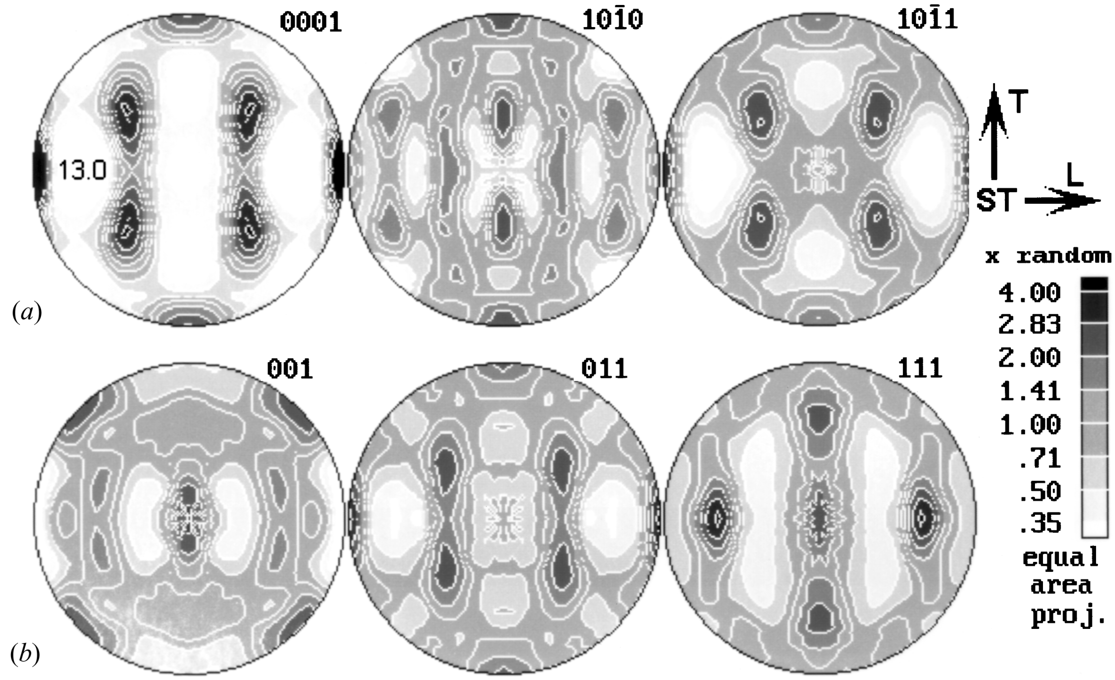

Fig. 1—Pole figures for Ti-6Al-4V with a colony alpha microstructure: (*a*) alpha phase and (*b*) beta phase.

In contrast to the research on aluminum and steels, relatively little effort has been expended to develop state-variable constitutive equations for two-phase, alpha + beta, titanium alloys such as Ti-6Al-4V. These materials are usually processed *via* an ingot metallurgy route comprising working and heat treatment in the single-phase beta field followed by breakdown in the alpha-beta field of the colony microstructure thus produced.[3] During this subtransus hot working, deformation is characterized by large amounts of flow softening and a gradual transition to a microstructure of globular alpha in a transformed-beta matrix. The occurrence of flow softening contrasts with the steady-state flow behavior exhibited by both single-phase alpha and single-phase beta titanium alloys.[4,5] Recently, a mechanism related to the loss of alpha-beta interface strength due to the development of microscopic shear bands within alpha lamellae has been proposed to explain the large degrees of flow softening developed during hot working of Ti-6Al-4V with a colony microstructure.[6] Calculations based on this model provided first-order agreement with measurements taken on samples cut from a highly textured Ti-6Al-4V plate deformed along different directions. However, the measurements did show a small, but non-negligible, anisotropy in the overall magnitude of flow softening with respect to test direction. Thus, the objective of the present work was to determine whether texture changes and the associated anisotropy in texture hardening or softening with test direction could explain the observed anisotropy in flow-softening behavior. This work would thus allow the separation of the effects of microstructure changes *per se* from those due to texture changes on constitutive behavior and therefore provide more accurate input for deformation models such as those based on the crystal-plasticity finite-element approach.

Previous experimental data on the flow-softening anisotropy of a Ti-6Al-4V plate material with a colony microstructure[6] served as the basis for the present investigation. The alpha-phase texture in this beta-heat-treated material (Figure 1(a)) had several components, the strongest of which was a rolling-direction basal component; the beta-phase texture (Figure 1(b)) consisted of a weak cube-on-face component. The flow behavior of the material had been determined *via* isothermal, hot compression tests conducted at a constant strain rate of 0.1 s^{-1} on samples whose compression axes were parallel to the rolling direction ("L"), long-transverse direction ("T"), 45 deg to the L and T directions ("45°"), or the short-transverse direction ("ST"). All of the flow curves exhibited a peak stress at low strains (~0.02) followed by extensive flow softening. A steady-state stress was reached by strains of the order of 0.70. The magnitude of flow softening was quantified by the index $\gamma = [\sigma_p - \sigma(0.65)]/\sigma_p$ in which σ_p and $\sigma(0.65)$ denote the peak flow stress (at a strain $\varepsilon \approx 0.02$) and the flow stress at a strain of 0.65, respectively.

The possible effect of texture hardening/softening on the observed flow-stress anisotropy was determined by conducting upper-bound (Taylor/Bishop–Hill) simulations of uniaxial compression using the Los Alamos polycrystal plasticity (LApp) computer code.[7] Although nonuniform deformation within grains/colonies and from grain to grain is overlooked in LApp, the program stills yields reasonable estimates of flow behavior provided the proper slip/twinning systems are used. All calculations were done for the alpha phase whose strength is several times that of the beta phase at hot-working temperatures[4,5] and thus should control the anisotropy in plastic flow. Inputs to these calculations included the measured texture of the alpha phase, the stress exponent for plastic flow *n* (taken to be 4.0), and various assumed ratios of the critical resolved shear stresses (CRSSs) for basal $\langle a \rangle$, prism $\langle a \rangle$, pyramidal $\langle c + a \rangle$, and pyramidal $\langle a \rangle$ slip. The alpha texture was described in terms of approximately 530 discrete crystal orientations weighted per the intensities in

Table I. **Measurements of the Flow Softening Index γ for Ti-6Al-4V with a Colony Microstructure***

Test Temperature (°C)	γ Along			
	L	T	45°	ST
815	0.444	0.400	0.346	0.353
900	0.461	0.430	0.368	0.385
955	0.365	0.331	0.292	0.308

*$\gamma = [\sigma_p - \sigma(\varepsilon = 0.65)]/\sigma_p$

the sample orientation distribution obtained from experimental data.[8] The CRSS ratio was taken to be constant for a given simulation; in essence, such an assumption is valid only if all slip systems soften (or harden) equally during large strain deformation. On the other hand, such simulations clearly elucidate the effect of texture changes *per se* on flow hardening/flow softening.[9] The principal outputs of the simulations were predictions of stress-strain (flow) curves and deformation textures. From the simulated flow curves, a flow softening/hardening index analogous to that used to quantity the measurements was derived, *i.e.*, $\gamma = [\sigma(0.02) - \sigma(0.65)]/\sigma(0.02)$, in which $\sigma(0.02)$ denotes the stress at a strain of 0.02.

Measured values of the flow-softening index γ for Ti-6Al-4V with the colony microstructure are summarized in Table I. All of the values were between 0.29 and 0.46, but there was a measurable dependence on test temperature and direction. The values for the two lower temperatures (815 °C and 900 °C) were higher by approximately 0.07 to 0.10 than those at the highest temperature. This is probably due to the fact that the volume fraction of alpha decreases from 0.83 to 0.50 to 0.20 at temperatures of 815 °C, 900 °C, and 955 °C. Thus, the flow-softening rate at the highest test temperature may be reduced by the large proportion of beta phase.

More importantly, the data in Table I reveal a dependence of γ on test direction that was similar at all three test temperatures. The values of γ were highest for testing along the rolling (L) direction and were successively lower for the T, ST, and 45° test directions. At a given test temperature, the difference in the L and 45° values of γ was approximately 0.10. Because of the absence of a noticeable *microstructural* texture in this material,[6] such an effect was ascribed to *crystallographic* texture. Moreover, the fact that the peak stresses were highest for the L direction and successively lower for the T, ST, and 45° directions[6] suggested that the crystallographic textures in all samples evolved to the same final texture. Indeed, pole-figure measurements after hot compression to a 50 pct height reduction did reveal similarly weak textures (maximum intensities were reduced from about 15 to 2.5 times random) for the different test directions. The *difference* in the flow-softening levels was thus concluded to be controlled by the effect of *initial* texture on the peak-stress anisotropy.

The first-order accuracy of LApp in simulating the alpha-phase texture evolution was verified by comparing predicted and measured textures; examples of this comparison are shown in Figure 2. The strongest peaks of the measured textures were consistent with the simulations, but the experimental data were much weaker. The differences may be

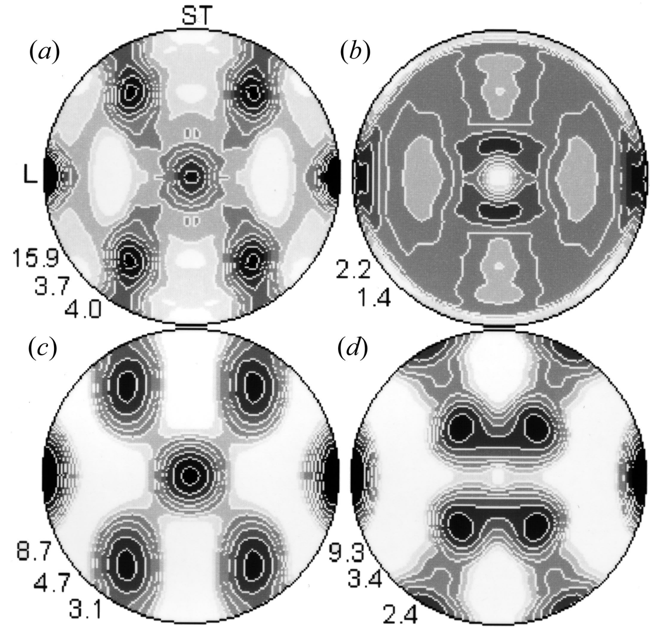

Fig. 2—Comparison of (*a*) and (*b*) measured and (*c*) and (*d*) smoothed, LApp-predicted (0001) pole figures; (*a*) and (*c*) are the textures of the undeformed sample, and (*b*) and (*d*) are textures after compression at 815 °C, 0.1 s^{-1} to a true strain of 0.7 along the T direction. Intensities of peaks are noted for the major texture components; (*a*), (*c*) and (*d*) use the same scale as Fig. 1, but contours for (*b*) are 0.59, 0.71, 0.84, 1.0, 1.19, 1.41, 1.68, and 2.0 due to weak intensity.

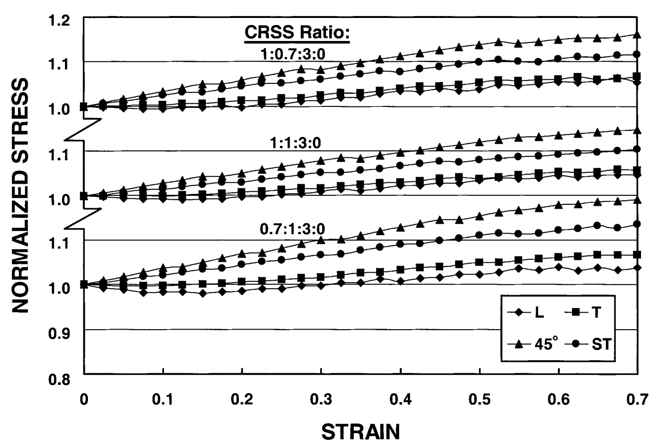

Fig. 3—Normalized stress-*vs*-strain plot for compression of Ti-6Al-4V along various directions as predicted by LApp assuming a CRSS ratio (basal $\langle a \rangle$:prism $\langle a \rangle$:pyramidal $\langle c + a \rangle$:pyramidal $\langle a \rangle$) of 1:0.7:3:0, 1:1:3:0, or 0.7:1:3:0.

partly attributed to the general trend of texture codes to predict sharper textures than observed.

Sample LApp predictions for the stress-strain curves of the Ti-6Al-4V alloy compressed along various directions are shown in Figure 3; the stresses have been normalized by the stress at zero strain. Results are shown for CRSS ratios of 1:0.7:3:0, 1:1:3:0, and 0.7:1:3:0 for basal $\langle a \rangle$, prism $\langle a \rangle$, pyramidal $\langle c + a \rangle$, and pyramidal $\langle a \rangle$ slip, respectively. In previous work,[6] the 1:0.7:3:0 ratio gave the best agreement between measured and predicted values of the peak stress and *r* values. In contrast to the measurements (Table I), however, the flow behavior predicted by LApp indicated

Table II. Texture Hardening Calculations for Ti-6Al-4V with a Colony Microstructure

CRSS Ratio				$-\gamma$			
Basal $\langle a\rangle$	Prism $\langle a\rangle$	Pyramidal $\langle c + a\rangle$	Pyramidal $\langle a\rangle$	L	T	45°	ST
1	0.5	2	—	0.058	0.050	0.095	0.070
1	0.7	3	—	0.060	0.072	0.144	0.103
1	1	3	—	0.048	0.054	0.135	0.095
0.7	1	3	—	0.045	0.067	0.175	0.128
0.3	1	2	3	0.029	0.027	0.170	0.123

Table III. Flow Softening Indices (γ*) for Ti-6Al-4V after Adjustment for Texture Hardening*

CRSS Ratio				γ*			
Basal $\langle a\rangle$	Prism $\langle a\rangle$	Pyramidal $\langle c + a\rangle$	Pyramidal $\langle a\rangle$	L	T	45°	ST
1	0.5	2	—	0.510	0.465	0.452	0.439
1	0.7	3	—	0.512	0.487	0.501	0.472
1	1	3	—	0.500	0.469	0.492	0.464
0.7	1	3	—	0.497	0.482	0.532	0.497
0.3	1	2	3	0.481	0.442	0.527	0.492

*Based on the average of γ's *measured* at 815 °C and 900 °C and texture hardening calculations in Table II.

a *hardening*, not softening, effect with increasing strain due to changes in crystallographic texture with deformation. This effect was seen consistently for all four test directions for the three sets of CRSS values in Figure 3.

LApp calculations of the flow hardening for several CRSS ratios are summarized in Table II. All of the values here are *negative* because the definition of γ leads to negative numbers for flow hardening and *positive* numbers for flow softening. The results in Table II show a marked dependence of hardening level on compression-test direction. For all of the CRSS ratios investigated, the predicted hardening was less for the L and T directions than for the 45° and ST directions.

The results in Tables I and II were combined to estimate the flow softening level that is not due to texture. For this purpose, attention was focused on the measurements at 815 °C and 900 °C at which the effect of alpha phase is strongest. For each test direction, the values of γ at these two temperatures were first averaged. This gave measured values of γ_{avg} of 0.452, 0.415, 0.357, and 0.369 for the L, T, 45°, and ST test directions, respectively. The computed values of the texture hardening index γ were subtracted from these γ_{avg}'s to obtain values of the true microstructural flow softening index γ*, which would be obtained in the absence of crystallographic-texture influences (Table III).

The microstructure-based flow softening index γ* (Table III) showed a much lower variation with compression-test direction. For the CRSS ratio of 1:0.7:3, found to be optimal previously for *r* value and peak stress predictions,[6] the maximum variation of γ* with test direction was found to be approximately 0.04, a value considerably smaller than that without correction for crystallographic texture changes (Table I). Further support for the argument that the remaining differences in γ* for the 1:0.7:3 ratio are not significant may be obtained from the almost identical values of γ* for the L and 45° directions, which are the two directions that exhibited the maximum difference in γ prior to adjustment for texture effects.

The CRSS ratio of 1:1:3:0 gave a similar result with respect to the limited variation of γ* with test direction (Table III). However, the other three values of the CRSS ratio in Table III reduced the γ* variation only to approximately 0.05 to 0.08. Hence, the value of the CRSS ratio, which previously provided the best indicator of peak stress anisotropy and *r* values, also appears to be useful in separating texture from microstructural influences on the flow softening observed in Ti-6Al-4V.

From this work, it is concluded that the anisotropy in flow softening rate observed when conducting upset tests along various directions of a textured plate can be ascribed to variations in the rate of texture hardening during deformation. Measured flow softening rates can be corrected using crystal-plasticity calculations to obtain the flow-softening rate due to microstructural effects alone. The CRSS ratio, which appears to give the best overall estimate of the effect of texture on plastic properties at hot working temperatures, is 1:0.7:3 for basal $\langle a\rangle$, prism $\langle a\rangle$, and pyramidal $\langle c + a\rangle$ slip, respectively.

This work was conducted as part of the in-house research activities of the Processing Science Group of the Air Force Research Laboratory's Materials and Manufacturing Directorate. The support and encouragement of the laboratory management and the Air Force Office of Scientific Research (Dr. C.S. Hartley, program manager) are gratefully acknowledged. One of the authors (TRB) was supported through Air Force Contract No. F33615-94-C-5804.

REFERENCES

1. C.M. Sellars and Q. Zhu: *Mater. Sci. Eng. A*, 2000, vol. A280, pp. 1-7.
2. R.L. Goetz and V. Seetharaman: *Scripta Mater.*, 1998, vol. 38, pp. 405-13.
3. S.L. Semiatin, V. Seetharaman, and I. Weiss: in *Advances in the Science and Technology of Titanium Alloy Processing*, I. Weiss, R. Srinivasan, P.J. Bania, D. Eylon, and S.L. Semiatin, eds., TMS, Warrendale, PA, 1997, pp. 3-73.

4. I. Weiss and S.L. Semiatin: *Mater. Sci. Eng. A*, 1999, vol. A263, pp. 243-56.
5. I. Weiss and S.L. Semiatin: *Mater. Sci. Eng. A*, 1998, vol. A243, pp. 46-65.
6. S.L. Semiatin and T.R. Bieler: *Metall. Mater. Trans. A*, 2001, vol. 32A, pp. 1787-99.
7. "Los Alamos Polycrystal Plasticity (LApp) Code," Report No. LA-CC-88-6, Los Alamos National Laboratory, Los Alamos, NM, 1988.
8. J.S. Kallend, U.F. Kocks, A.D. Rollett, and H.-R. Wenk: *Mater. Sci. Eng. A*, 1991, vol. A132, pp. 1-11.
9. R.M. Miller, T.R. Bieler, and S.L. Semiatin: *Scripta Mater.*, 1999, vol. 40, pp. 1387-93.